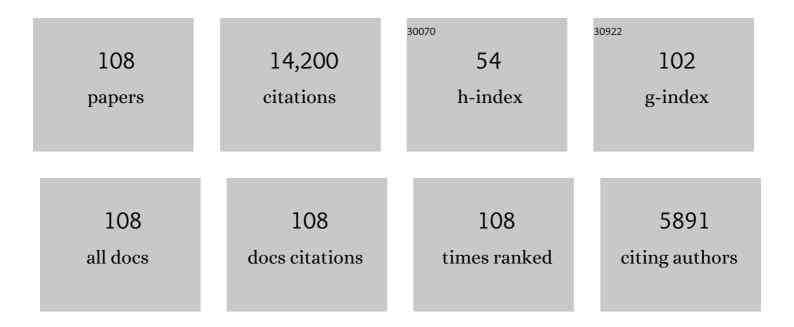
Tom Theuns

List of Publications by Year in descending order

Source: https://exaly.com/author-pdf/4210833/publications.pdf Version: 2024-02-01



#	Article	IF	CITATIONS
1	The origin of correlations between mass, metallicity, and morphology in galaxies from the <scp>eagle</scp> simulation. Monthly Notices of the Royal Astronomical Society, 2022, 512, 6164-6179.	4.4	5
2	The evolution of the oxygen abundance gradients in star-forming galaxies in the <scp>eagle</scp> simulations. Monthly Notices of the Royal Astronomical Society, 2022, 511, 1667-1684.	4.4	12
3	MUSE analysis of gas around galaxies (MAGG) – III. The gas and galaxy environment of <i>z</i> = 3–4.5 quasars. Monthly Notices of the Royal Astronomical Society, 2021, 503, 3044-3064.	4.4	40
4	Smoothed particle radiation hydrodynamics: two-moment method with local Eddington tensor closure. Monthly Notices of the Royal Astronomical Society, 2021, 505, 5784-5814.	4.4	9
5	Metal-enriched halo gas across galaxy overdensities over the last 10 billion years. Monthly Notices of the Royal Astronomical Society, 2021, 508, 4573-4599.	4.4	30
6	The surprising accuracy of isothermal Jeans modelling of self-interacting dark matter density profiles. Monthly Notices of the Royal Astronomical Society, 2021, 501, 4610-4634.	4.4	34
7	Correlations between mass, stellar kinematics, and gas metallicity in eagle galaxies. Monthly Notices of the Royal Astronomical Society: Letters, 2020, 496, L33-L37.	3.3	4
8	Infrared luminosity functions and dust mass functions in the EAGLE simulation. Monthly Notices of the Royal Astronomical Society, 2020, 494, 2912-2924.	4.4	16
9	Measuring the temperature and profiles of Ly α absorbers. Monthly Notices of the Royal Astronomical Society, 2020, 492, 2193-2207.	4.4	8
10	From peculiar morphologies to Hubble-type spirals: the relation between galaxy dynamics and morphology in star-forming galaxies at z â^¼ 1.5. Monthly Notices of the Royal Astronomical Society, 2020, 492, 1492-1512.	4.4	11
11	Connecting cosmological accretion to strong Ly α absorbers. Monthly Notices of the Royal Astronomical Society, 2020, 500, 2741-2756.	4.4	12
12	Linking gas and galaxies at high redshift: MUSE surveys the environments of six damped Lyα systems at z â‰^ 3. Monthly Notices of the Royal Astronomical Society, 2019, 487, 5070-5096.	4.4	33
13	The MUSE Ultra Deep Field (MUDF). II. Survey design and the gaseous properties of galaxy groups at 0.5 < z < 1.5. Monthly Notices of the Royal Astronomical Society, 2019, 490, 1451-1469.	4.4	38
14	The nature of submillimetre and highly star-forming galaxies in the EAGLE simulation. Monthly Notices of the Royal Astronomical Society, 2019, 488, 2440-2454.	4.4	50
15	The dynamics and distribution of angular momentum in HiZELS star-forming galaxies at <i>z</i> Â=Â0.8–3.3. Monthly Notices of the Royal Astronomical Society, 2019, 486, 175-194.	4.4	17
16	Fluorescent rings in star-free dark matter haloes. Monthly Notices of the Royal Astronomical Society, 2019, 487, 609-621.	4.4	5
17	The cosmic spectral energy distribution in the EAGLE simulation. Monthly Notices of the Royal Astronomical Society, 2019, 484, 4069-4082.	4.4	17
18	Disruption of satellite galaxies in simulated groups and clusters: the roles of accretion time, baryons, and pre-processing. Monthly Notices of the Royal Astronomical Society, 2019, 485, 2287-2311.	4.4	47

#	Article	IF	CITATIONS
19	The MUSE Ultra Deep Field (MUDF) – I. Discovery of a group of Lyα nebulae associated with a bright <i>z</i> Ââ‰^Â3.23 quasar pair. Monthly Notices of the Royal Astronomical Society: Letters, 2019, 485, L62-L67.	3.3	18
20	The relationship between the morphology and kinematics of galaxies and its dependence on dark matter halo structure in EAGLE. Monthly Notices of the Royal Astronomical Society, 2019, 485, 972-987.	4.4	59
21	The oxygen abundance gradients in the gas discs of galaxies in the EAGLE simulation. Monthly Notices of the Royal Astronomical Society, 2019, 482, 2208-2221.	4.4	49
22	The star formation rate and stellar content contributions of morphological components in the EAGLE simulations. Monthly Notices of the Royal Astronomical Society, 2019, 483, 744-766.	4.4	47
23	The evolution of the baryon fraction in haloes as a cause of scatter in the galaxy stellar mass in the <scp>eagle</scp> simulation. Monthly Notices of the Royal Astronomical Society, 2019, 482, 3261-3273.	4.4	13
24	Galaxies with monstrous black holes in galaxy cluster environments. Monthly Notices of the Royal Astronomical Society, 2019, 485, 396-407.	4.4	14
25	An Evolving and Mass-dependent σsSFR–M _⋆ Relation for Galaxies. Astrophysical Journal, 2019, 879, 11.	4.5	24
26	The chemical imprint of the bursty nature of Milky Way's progenitors. Monthly Notices of the Royal Astronomical Society: Letters, 2019, 482, L145-L149.	3.3	3
27	Comparing galaxy formation in semi-analytic models and hydrodynamical simulations. Monthly Notices of the Royal Astronomical Society, 2018, 474, 492-521.	4.4	42
28	The innate origin of radial and vertical gradients in a simulated galaxy disc. Monthly Notices of the Royal Astronomical Society, 2018, 476, 3648-3660.	4.4	26
29	Origins of carbon-enhanced metal-poor stars. Monthly Notices of the Royal Astronomical Society, 2018, 473, 984-995.	4.4	16
30	Quantifying the impact of mergers on the angular momentum of simulated galaxies. Monthly Notices of the Royal Astronomical Society, 2018, 473, 4956-4974.	4.4	113
31	The rapid growth phase of supermassive black holes. Monthly Notices of the Royal Astronomical Society, 2018, 481, 3118-3128.	4.4	58
32	The origin of diverse α-element abundances in galaxy discs. Monthly Notices of the Royal Astronomical Society, 2018, 477, 5072-5089.	4.4	77
33	The Cluster-EAGLE project: velocity bias and the velocity dispersion–mass relation of cluster galaxies. Monthly Notices of the Royal Astronomical Society, 2018, 474, 3746-3759.	4.4	33
34	Knowing the unknowns: uncertainties in simple estimators of galactic dynamical masses. Monthly Notices of the Royal Astronomical Society, 2017, 469, 2335-2360.	4.4	54
35	Angular momentum evolution of galaxies in EAGLE. Monthly Notices of the Royal Astronomical Society, 2017, 464, 3850-3870.	4.4	126
36	The EAGLE simulations: atomic hydrogen associated with galaxies. Monthly Notices of the Royal Astronomical Society, 2017, 464, 4204-4226.	4.4	130

#	Article	IF	CITATIONS
37	Size matters: abundance matching, galaxy sizes, and the Tully–Fisher relation in EAGLE. Monthly Notices of the Royal Astronomical Society, 2017, 464, 4736-4746.	4.4	43
38	Mass-Discrepancy Acceleration Relation: A Natural Outcome of Galaxy Formation in Cold Dark Matter Halos. Physical Review Letters, 2017, 118, 161103.	7.8	95
39	The dark nemesis of galaxy formation: why hot haloes trigger black hole growth and bring star formation to an end. Monthly Notices of the Royal Astronomical Society, 2017, 465, 32-44.	4.4	214
40	The low-mass end of the baryonic Tully–Fisher relation. Monthly Notices of the Royal Astronomical Society, 2017, 464, 2419-2428.	4.4	69
41	Optical colours and spectral indices of zÂ=Â0.1 eagle galaxies with the 3D dust radiative transfer code skirt. Monthly Notices of the Royal Astronomical Society, 2017, 470, 771-799.	4.4	152
42	Small-scale galaxy clustering in the eagle simulation. Monthly Notices of the Royal Astronomical Society, 2017, 470, 1771-1787.	4.4	28
43	A comparison of observed and simulated absorption from H <scp>i</scp> , C <scp>iv</scp> , and Si <scp>iv</scp> around <i>z</i> ≠ 2 star-forming galaxies suggests redshift–space distortions are to inflows. Monthly Notices of the Royal Astronomical Society, 2017, 471, 690-705.	duae	62
44	Witnessing galaxy assembly in an extended zâ‰^3 structure. Monthly Notices of the Royal Astronomical Society, 2017, 471, 3686-3698.	4.4	41
45	The evolution of the star formation rate function in the EAGLE simulations: a comparison with UV, IR and Hα observations from z â^¼ 8 to z â^¼ 0. Monthly Notices of the Royal Astronomical Society, 2017, 472, 919-939.	4.4	62
46	The relation between galaxy morphology and colour in the EAGLE simulation. Monthly Notices of the Royal Astronomical Society: Letters, 2017, 472, L45-L49.	3.3	71
47	Galaxy metallicity scaling relations in the EAGLE simulations. Monthly Notices of the Royal Astronomical Society, 2017, 472, 3354-3377.	4.4	98
48	Size evolution of normal and compact galaxies in the EAGLE simulation. Monthly Notices of the Royal Astronomical Society, 2017, 465, 722-738.	4.4	170
49	The origin of scatter in the stellar mass–halo mass relation of central galaxies in the EAGLE simulation. Monthly Notices of the Royal Astronomical Society, 2017, 465, 2381-2396.	4.4	100
50	Finding the stars that reionized the Universe. Proceedings of the International Astronomical Union, 2017, 12, 253-254.	0.0	0
51	The origin of the enhanced metallicity of satellite galaxies. Monthly Notices of the Royal Astronomical Society, 2017, 464, 508-529.	4.4	36
52	A chronicle of galaxy mass assembly in the EAGLE simulation. Monthly Notices of the Royal Astronomical Society, 2017, 464, 1659-1675.	4.4	145
53	The Fundamental Plane of star formation in galaxies revealed by the EAGLE hydrodynamical simulations. Monthly Notices of the Royal Astronomical Society, 2016, 459, 2632-2650.	4.4	84
54	Galaxies in the EAGLE hydrodynamical simulation and in the Durham and Munich semi-analytical models. Monthly Notices of the Royal Astronomical Society, 2016, 461, 3457-3482.	4.4	85

Tom Theuns

#	Article	IF	CITATIONS
55	MUSE searches for galaxies near very metal-poor gas clouds at <i>z</i> â^1⁄4 3: new constraints for cold accretion models. Monthly Notices of the Royal Astronomical Society, 2016, 462, 1978-1988.	4.4	66
56	The environmental dependence of H i in galaxies in the eagle simulations. Monthly Notices of the Royal Astronomical Society, 2016, 461, 2630-2649.	4.4	77
57	The APOSTLE simulations: solutions to the Local Group's cosmic puzzles. Monthly Notices of the Royal Astronomical Society, 2016, 457, 1931-1943.	4.4	453
58	The effect of baryons on redshift space distortions and cosmic density and velocity fields in the EAGLE simulation. Monthly Notices of the Royal Astronomical Society: Letters, 2016, 461, L11-L15.	3.3	75
59	The link between the assembly of the inner dark matter halo and the angular momentum evolution of galaxies in the EAGLE simulation. Monthly Notices of the Royal Astronomical Society, 2016, 460, 4466-4482.	4.4	86
60	The eagle simulations of galaxy formation: Public release of halo and galaxy catalogues. Astronomy and Computing, 2016, 15, 72-89.	1.7	394
61	Towards the statistical detection of the warm–hot intergalactic medium in intercluster filaments of the Royal Astronomical Society, 2016, 455, 2662-2697.	4.4	31
62	Bent by baryons: the low-mass galaxy-halo relation. Monthly Notices of the Royal Astronomical Society, 2015, 448, 2941-2947.	4.4	163
63	The impact of angular momentum on black hole accretion rates in simulations of galaxy formation. Monthly Notices of the Royal Astronomical Society, 2015, 454, 1038-1057.	4.4	219
64	Colours and luminosities of <i>z</i> Â=Â0.1 galaxies in the eagle simulation. Monthly Notices of the Royal Astronomical Society, 2015, 452, 2879-2896.	4.4	200
65	The eagle simulations of galaxy formation: the importance of the hydrodynamics scheme. Monthly Notices of the Royal Astronomical Society, 2015, 454, 2277-2291.	4.4	192
66	Evolution of galaxy stellar masses and star formation rates in the eagle simulations. Monthly Notices of the Royal Astronomical Society, 2015, 450, 4486-4504.	4.4	332
67	The distribution of neutral hydrogen around high-redshift galaxies and quasars in the EAGLE simulation. Monthly Notices of the Royal Astronomical Society, 2015, 452, 2034-2056.	4.4	124
68	The EAGLE simulations of galaxy formation: calibration of subgrid physics and model variations. Monthly Notices of the Royal Astronomical Society, 2015, 450, 1937-1961.	4.4	1,038
69	The alignment and shape of dark matter, stellar, and hot gas distributions in the EAGLE and cosmo-OWLS simulations. Monthly Notices of the Royal Astronomical Society, 2015, 453, 721-738.	4.4	108
70	The EAGLE project: simulating the evolution and assembly of galaxies and their environments. Monthly Notices of the Royal Astronomical Society, 2015, 446, 521-554.	4.4	2,549
71	The broadening of Lyman-α forest absorption lines. Monthly Notices of the Royal Astronomical Society, 2015, 450, 1465-1476.	4.4	31
72	Baryon effects on the internal structure of $\hat{\mathbf{b}}$ CDM haloes in the EAGLE simulations. Monthly Notices of the Royal Astronomical Society, 2015, 451, 1247-1267.	4.4	302

#	Article	IF	CITATIONS
73	Galaxy properties and the cosmic web in simulations. Monthly Notices of the Royal Astronomical Society, 2015, 446, 1458-1468.	4.4	33
74	A compact, metal-rich, kpc-scale outflow in FBQS J0209â^'0438: detailed diagnostics from HST/COS extreme UV observations. Monthly Notices of the Royal Astronomical Society, 2014, 440, 3317-3340.	4.4	28
75	The VLT LBG Redshift Survey – III. The clustering and dynamics of Lyman-break galaxies at z â^1⁄4 3â~ Monthly Notices of the Royal Astronomical Society, 2013, 430, 425-449.	4.4	56
76	Physical properties of simulated galaxy populations at $z = 2$ â \in "II. Effects of cosmology, reionization and ISM physics. Monthly Notices of the Royal Astronomical Society, 2013, 435, 2955-2967.	4.4	27
77	The impact of different physical processes on the statistics of Lyman-limit and damped Lyman $\hat{I}\pm$ absorbers. Monthly Notices of the Royal Astronomical Society, 2013, 436, 2689-2707.	4.4	40
78	How supernova explosions power galactic winds. Monthly Notices of the Royal Astronomical Society, 2013, 429, 1922-1948.	4.4	131
79	Physical properties of simulated galaxy populations at z = 2 – I. Effect of metal-line cooling and feedback from star formation and AGN. Monthly Notices of the Royal Astronomical Society, 2013, 435, 2931-2954.	4.4	59
80	urchin: a reverse ray tracer for astrophysical applications. Monthly Notices of the Royal Astronomical Society, 2013, 434, 748-764.	4.4	29
81	The phase-space density of fermionic dark matter haloes. Monthly Notices of the Royal Astronomical Society, 2013, 430, 2346-2357.	4.4	84
82	THE PROPERTIES OF THE STAR-FORMING INTERSTELLAR MEDIUM AT <i>z</i> = 0.8–2.2 FROM HiZELS: STAR FORMATION AND CLUMP SCALING LAWS IN GAS-RICH, TURBULENT DISKS. Astrophysical Journal, 2012, 760, 130.	4.5	120
83	The properties of the star-forming interstellar medium at <i>z</i> = 0.84-2.23 from HiZELS: mapping the internal dynamics and metallicity gradients in high-redshift disc galaxies. Monthly Notices of the Royal Astronomical Society, 2012, 426, 935-950.	4.4	139
84	Cold accretion flows and the nature of high column density H i absorption at redshift 3. Monthly Notices of the Royal Astronomical Society, 2012, 421, 2809-2819.	4.4	126
85	The Aquila comparison project: the effects of feedback and numerical methods on simulations of galaxy formation. Monthly Notices of the Royal Astronomical Society, 2012, 423, 1726-1749.	4.4	381
86	Large-scale structure in absorption: gas within and around galaxy voids. Monthly Notices of the Royal Astronomical Society, 2012, 425, 245-260.	4.4	25
87	THROUGH THICK AND THIN—H I ABSORPTION IN COSMOLOGICAL SIMULATIONS. Astrophysical Journal Letters, 2011, 737, L37.	8.3	115
88	The VLT LBG Redshift Survey☠II. Interactions between galaxies and the IGM at z∼ 3. Monthly Notices of the Royal Astronomical Society, 2011, 414, 28-49.	4.4	52
89	Mismatch and misalignment: dark haloes and satellites of disc galaxies. Monthly Notices of the Royal Astronomical Society, 2011, 415, 2607-2625.	4.4	107
90	Cosmological simulations of the formation of the stellar haloes around disc galaxies. Monthly Notices of the Royal Astronomical Society, 2011, 416, 2802-2820.	4.4	232

#	Article	IF	CITATIONS
91	The stellar and hot gas content of low-mass galaxy clusters. Monthly Notices of the Royal Astronomical Society, 2010, , no-no.	4.4	2
92	The physics driving the cosmic star formation history. Monthly Notices of the Royal Astronomical Society, 2010, 402, 1536-1560.	4.4	704
93	The properties of satellite galaxies in simulations of galaxy formation. Monthly Notices of the Royal Astronomical Society, 2010, 406, 208-222.	4.4	137
94	Cosmological radiative transfer comparison project – II. The radiation-hydrodynamic tests. Monthly Notices of the Royal Astronomical Society, 2009, 400, 1283-1316.	4.4	94
95	Chemical enrichment in cosmological, smoothed particle hydrodynamics simulations. Monthly Notices of the Royal Astronomical Society, 2009, 399, 574-600.	4.4	525
96	Mass loss of galaxies due to an ultraviolet background. Monthly Notices of the Royal Astronomical Society, 2008, 390, 920-928.	4.4	443
97	The halo mass function from the dark ages through the present day. Monthly Notices of the Royal Astronomical Society, 2007, 374, 2-15.	4.4	298
98	Simulating the ionisation and metal enrichment history of the intergalactic medium. Proceedings of the International Astronomical Union, 2005, 1, 308-312.	0.0	0
99	The mean HI optical depth of the intergalactic medium. Proceedings of the International Astronomical Union, 2005, 1, 397-399.	0.0	0
100	Numerical simulations of quasar absorbers. Proceedings of the International Astronomical Union, 2005, 1, 185-204.	0.0	2
101	ELT requirements for future observations of the Intergalactic Medium. Proceedings of the International Astronomical Union, 2005, 1, 464-471.	0.0	0
102	The first generation of star-forming haloes. Monthly Notices of the Royal Astronomical Society, 2005, 363, 393-404.	4.4	56
103	Dark energy effects on the Lyman forest. Monthly Notices of the Royal Astronomical Society, 2003, 340, L47-L51.	4.4	22
104	Metallicity of the Intergalactic Medium Using Pixel Statistics. II. The Distribution of Metals as Traced by Civ. Astrophysical Journal, 2003, 596, 768-796.	4.5	338
105	P3M-SPH simulations of the Lyα forest. Monthly Notices of the Royal Astronomical Society, 1998, 301, 478-502.	4.4	318
106	Evolution of the angular momentum of protogalaxies from tidal torques: Zel'dovich approximation. Monthly Notices of the Royal Astronomical Society, 1996, 282, 436-454.	4.4	179
107	The ll̊ºl̂µl̂± model of feedback-regulated galaxy formation. Monthly Notices of the Royal Astronomical Society, 0, , .	4.4	12
108	MUSE searches for galaxies near very metal-poor gas clouds at z â^1⁄4 3: new constraints for cold accretion models. , 0, .		1

7